Jet measurements in future e+A colliders

The EIC e+A working group

November 2008

Abstract

In this note, we describe the measurements that one can perform at the future EIC colliders based on jets in the final state. We put emphasis on observables that are unique to the heavy-ion case and provide valuable information on the structure of the nucleus.

Contents

1 Jet measurements **2**

2 Generic DIS kinematics **2**

3 Jet reconstruction in DIS **3**

4 Gluon distribution from 2+1 jets **5**

4.1 Kinematics 5
4.2 Extraction of the gluon distribution 8
4.3 Simulations and expected statistical errors 11
4.4 Systematic errors 13
4.5 Conclusions and discussion 14

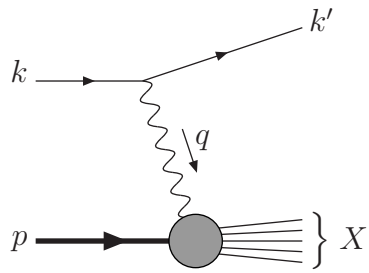

Figure 1: Generic kinematics of a DIS process.

1 Jet measurements

Give a list of the interesting measurements that one can do using jets, put special emphasis on the ones that are specific to the eA situation

- **Jet quenching in cold medium**:
- **Gluon distribution from 2+1-jet**:

Speak about what has been done at HERA

2 Generic DIS kinematics

Let us start the discussion by introducing the kinematic variables that we shall use. Since a significant part of the discussion in this note concerns the regions of phase-space that will hopefully be reached, we shall discuss later on (see *e.g.* Section 4.1) the influence of various cuts we can put on the different kinematic variables we introduce here.

We first introduce the traditional DIS variables (neglecting the beam masses)

$$s = (p+k)^2, \tag{1}$$

$$W^2 = (p+q)^2, \tag{2}$$

$$Q^2 = -q^2, \tag{3}$$

$$x = \frac{Q^2}{2p.q} = \frac{Q^2}{W^2+Q^2}, \tag{4}$$

$$y = \frac{p.q}{p.k} = \frac{Q^2}{sx}, \tag{5}$$

where k, p and q are the momenta of the incoming lepton, incoming proton and exchanged virtual photon respectively.

Experimentally, we will have asymmetric collisions the laboratory frame. If we denote by P and E the energy of the proton and lepton beam and by k' the outgoing lepton of energy E' and scattering angle θ, we have

$$p \equiv (0, 0, P, P), \tag{6}$$
$$k \equiv (0, 0, -E, E), \tag{7}$$
$$k' \equiv (E' \sin(\theta), 0, -E' \cos(\theta), E'). \tag{8}$$

The kinematic variables introduced here-above can thus be directly computed by only measuring the energy and scattering angle of the outgoing electron:

$$s = 4EP, \tag{9}$$
$$W^2 = 4EP - 2E' \left[P + E + (P - E)\cos(\theta)\right], \tag{10}$$
$$Q^2 = 2EE' \left[1 - \cos(\theta)\right], \tag{11}$$
$$x = \frac{EE' \left[1 - \cos(\theta)\right]}{2EP - E'P \left[1 + \cos(\theta)\right]}. \tag{12}$$

3 Jet reconstruction in DIS

Before discussing the physical measurements involving jets that we plan to study at the EIC, we will make a few generic comments on jet clustering in DIS experiments.

The first important point is that, in a vast majority of cases, the jet reconstruction is conducted in the Breit frame. The latter is defined as the frame where the proton moves along the positive z direction, the virtual photon along the negative z direction and has a vanishing energy. In other words, the only non-zero component of the photon momentum is $q_z = -Q$ and, as a consequence, the longitudinal momentum of the proton will be $p_z = Q/(2x)$.

The Breit frame is often seen as a natural choice to study the final state of a hard scattering. The first reason for that is that a hard parton coming out of the proton carries, in the Breit frame, a momentum $p_z = Q/2$. The Breit frame is thus (nearly) the centre-of-mass frame for the partonic interaction. The fact that it is not exactly the partonic centre-of-mass frame — in which the incoming parton would carry a momentum $p_z = Q$ — is actually the main motivation for using the Breit frame. Because of the small asymmetry

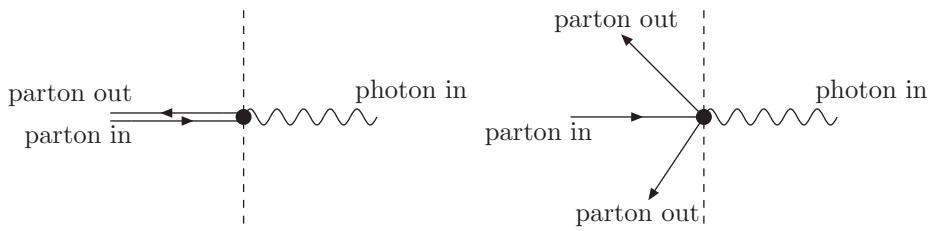

(a) LO scattering in the Breit frame (b) NLO scattering in the Breit frame

Figure 2: Scattering in the Breit frame at the two lowest orders of the perturbation theory. The photon comes from the negative z axis and the incoming parton from the positive z axis.

of the collision, the particles produced will tend to populate the region of negative z momentum while the beam remnants will carry on with positive z momentum. The Breit frame thus allows for a clear separation between the products of the hard partonic interaction and the beam remnants. This is illustrated in Fig. 2, first at lowest order of the perturbation theory (Fig. 2(a)) where the final state is just a single parton going back along the negative z direction with momentum $p_z = -Q/2$, and then at the next order (Fig. 2(b)) where we have two partons in the final state. Note that in this last case, the two ooutgoing partons will have opposite transverse momentum.

Another thing one needs to notice is that the boost required to go from the laboratory frame to the Breit frame depends on x and Q^2 and will thus vary from one event to another. As a consequence, even if one has a clear separation between the proton and the results of the hard scattering in the Breit frame, this distinction might not be as clear in the laboratory frame. In certain regions of the phase-space, this can also become an experimental issue. Indeed, boosting the particles from the laboratory frame to the Breit frame might amplify the uncertainties on the determination of their momentum. For example, at small values of x, one needs to be aware that a large boost in the longitudinal direction is required. Conversely, at large x, the partonic system appears very close to the beam remnants in the laboratory frame, therefore, if the two are not well distinguished because of experimental precision in the laboratory frame, that will still be the case in the Breit frame.

Since jet analysis are usually interested in the jets resulting from the

partonic interaction, it is natural to cluster the particles in the Breit fram[1]. For that reasons, one usually labels an event as "n+1 jets" if it has n jets coming from the hard partonic interaction, the "+1" standing for the beam remnants. The lowest order diagram (Fig. 2(a)) is thus a 1+1-jet event, while the one corresponding to Fig. 2(b) will always be a 2+1-jet event as the outgoing partons have opposite transverse momenta.

The last point we need to discuss is the choice of the jet definition used to perform the clustering. DIS events are usually reasonably quiet events with low multiplicities, much closer to the multiplicities obtained in e^+e^- collisions than to the ones reached in pp collisions. As a consequence, one usually uses the longitudinally-invariant k_t algorithm [3] with a distance parameter $R = 1$ to cluster the final-state particles. This algorithm is known to be well-suited for perturbative computations and QCD resummations and is thus often preferred to cone-type algorithms which have a more complicated perturbative nehaviour and a a lower sensitivity to soft-radiation, making them more justified at larger multiplicities.

4 Gluon distribution from 2+1 jets

4.1 Kinematics

As already emphasised, an important part of our concerns in the extraction of the gluon distributino from jet measurements will be to figure out the accessible regions of the phase-space. We shall thus begin our study with a discussion of the kinematical variables introduced in Section 2 and, more specifically, of the cuts one usually has to apply on these variables. Since these are the variables that are the most commonly used, we will consider the available phase-space in x and Q^2.

The first constraint is comes directly from (11) and the fact that the energy of the outgoing lepton cannot be larger that the one of the incoming lepton leading to $0 \leq Q^2 \leq 4EE' \leq 4E^2$. As a consequence, we realise that in order to reach large values of Q^2, we need back-scattered leptons (*i.e.* large values of θ) with a large energy.

One of the constraints that will play a major role when we will discuss the region of the phase-space where we should be able to extract the gluon density, is the cut on the outgoing electron energy. In practice, it is not possible to efficiently detect electrons above a threshold energy E_{cut} (we

[1]Though the clustering will be performed using a longitudineally invariant algorithm, going from the laboratory frame to the Breit freame requires a boost and a rotation, hence the result of the clustering will be different in the two frames.

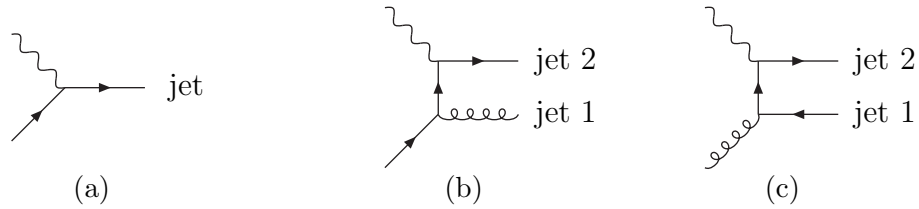

Figure 3: Parton-level processes that contribute (a) to the 1+1 and (b,c) 2+1 jet cross-section.

shall discuss practical values for this cut later on). Using (11), we can get rid of θ in (12), leading to

$$x = \frac{Q^2}{4P\left(E - E' + \frac{Q^2}{4E}\right)}.$$

We thus see that if we want to reach small values of x we want to minimise the energy of the outgoing electron. Without the experimental cut on E', the minimal value we can reach is $Q^2/(4E)$, obtained from (11) when θ is large, corresponding to $x_{\min} = Q^2/(4PE)$. This is the common bound where as Q^2 decreases one has access to smaller and smaller values of x. This is reminiscent of the fact that small x tends to prefer small outgoing electron energies which also suggests small Q^2. Once we also take into account the cut on the outgoing electron energy, we have

$$x \geq \frac{Q^2}{4P\left(E - E_0 + \frac{Q^2}{4E}\right)}, \tag{13}$$

with $E_0 = \max(E_{\text{cut}}, Q^2/(4E))$. At small values of Q^2, the minimal accessible x is thus slightly shifted towards higher values.

We also need to mention the fact that going to small x while keeping Q^2 large enough means going to values of θ as large as possible. In that case, the scattered electron hits the detector on the proton side, meaning that it might be difficult experimentally to detect it in the middle of the proton-beam remnants. For those reasons, a cut $\theta_{\max}$ is sometimes applied. Its effect is similar to a cut on E' so we will not discuss this option here.

Let us now turn to the more specific case of jets in the final state. At lowest order of the perturbation theory, the virtual photon scatters from a quark directly coming from the proton as depicted in Figure **to be filled**. As discussed in Section 3, that lowest-order configuration is a 1+1 jet *i.e.*

one jet from the proton remnants and one from the hard scattering. We shall argue in the next section that jets become interesting to extract the gluon distribution at the next order. There are two contributions to the $\mathcal{O}(\alpha_s)$ corrections: a quark-initiated process with a gluon and a quark in the final state, and a gluon-initiated process with a quark-antiquark pair in the final state. In the Breit frame, these contributions will give rise to two jets back-to-back in azimuth and well separated from the proton beam remnants.

The whole idea behind the extraction of the gluon density is to identify these configurations with 2+1 jets and use them to reconstruct the incoming parton. If one finds a way to isolate the contribution from the gluon-initiated processes from the quark-initiated ones, this would give a direct access to the gluon density.

Practically speaking, if the incoming parton carries a fraction x_p of the proton's longitudinal momentum (we shall also use x_g in the case of a gluon)m the centre-of-mass energy of the photon-incoming parton system is $\hat{s} = (x_p p + q)^2$, from which one easily gets

$$x_p = x\left(1 + \frac{\hat{s}}{Q^2}\right). \tag{14}$$

This is where the jet analysis of the final state will become the most interesting: by identifying these 2+1-jet situations, we can reconstruct $\hat{s}$ which is also the invariant mass of the dijet system, hence get access to x_p. The system is thus fully specified by x and Q^2, obtained from the outgoing electron, and $\hat{s}$ computed from the final state.

At the level of the kinematic, the one cut we need to discuss is a $p_{t,\mathrm{cut}}$ cut on the jets transverse momentum. The main motivation for this cut is to ensure a clean separation between the "hard" jets coming from the partonic interaction and the softer jets coming from the proton remains. Since this cut will be imposed in the Breit frame where the jets go in opposite directions, we have $\hat{s} \geq 4p_{t,\mathrm{cut}}^2$. From (13) and (14) we deduce the lower limit of the accessible value of x_p

$$x_p \geq \frac{Q^2 E}{P\left[Q^2 + 4E(E - E_0)\right]}\left(1 + \frac{4p_{t,\mathrm{cut}}^2}{Q^2}\right) \quad \text{with} \quad E_0 = \max\left(E_{\mathrm{cut}}, \frac{Q^2}{4E}\right). \tag{15}$$

It is interesting to note that, to the contrary of the lowest bound on x, there is a fixed limit on x_p at small Q^2

$$x_p \geq \frac{p_{t,\mathrm{cut}}^2}{P(E - E_{\mathrm{cut}})}, \tag{16}$$

coming from the fact that at small Q^2 it becomes increasingly difficult to pass the $p_{t,\mathrm{cut}}$ threshold.

4.2 Extraction of the gluon distribution

In this Section, we describe the method we suggest in order to extract the gluon distribution from the 2+1-jet cross-section. We also emphasise in what respect this could provide an information complementary (or even better) than the traditional extraction of the gluon distribution through DGLAP fit to the inclusive cross-section.

In the case of the inclusive measurements of the proton (or nuclear) structure functions, the quark and gluon parton distribution functions (PDF) are extracted through a DGLAP evolution [1]. This means that one has to solve the following set of equations[2]

$$\begin{aligned} Q^2\partial_{Q^2}\Sigma(x,Q^2) &= \int_x^1 \frac{d\xi}{\xi} P_{qq}\left(\frac{x}{\xi},\alpha_s\right)\Sigma(\xi,Q^2) + 2n_f P_{qg}\left(\frac{x}{\xi},\alpha_s\right) g(\xi,Q^2), \\ Q^2\partial_{Q^2} g(x,Q^2) &= \int_x^1 \frac{d\xi}{\xi} P_{gq}\left(\frac{x}{\xi},\alpha_s\right)\Sigma(\xi,Q^2) + P_{gg}\left(\frac{x}{\xi},\alpha_s\right) g(\xi,Q^2), \end{aligned} \tag{17}$$

where we have introduced the singlet distribution $\Sigma(x,Q^2) = \sum_q (q+\bar{q})$, and the splitting functions $P_{ab}(x,\alpha_s)$ that can be computed perturbatively in QCD

$$P_{ab}(x,\alpha_s) = \frac{\alpha_s}{2\pi} P^{(0)}(x) + \left(\frac{\alpha_s}{2\pi}\right)^2 P^{(1)}(x) + \dots \tag{18}$$

and are known so far at NNLO *i.e.* at $\mathcal{O}(\alpha_s^3)$ [2].

The structure functions are then related to the parton distribution functions by convolution through the Wilson coefficients:

$$F_2(x,Q^2) = \int \frac{d\xi}{\xi}\left[\sum_q C_q\left(\frac{x}{\xi},\alpha_s\right)(q+\bar{q})(\xi,Q^2) + C_g\left(\frac{x}{\xi},\alpha_s\right) g(\xi,Q^2)\right] \tag{19}$$

where, as for the splitting functions, the Wilson coefficients can be computed in perturbative theory

$$C_q(x,\alpha_s) = e_q^2 x\delta(1-x) + \frac{\alpha_s}{2\pi} C_q^{(1)}(x) + \dots \tag{20}$$

$$C_q(x,\alpha_s) = \frac{\alpha_s}{2\pi} C_g^{(1)}(x) + \dots \tag{21}$$

[2] We omit other flavour non-singlet combinations of the quark distributions that do not couple to the gluon.

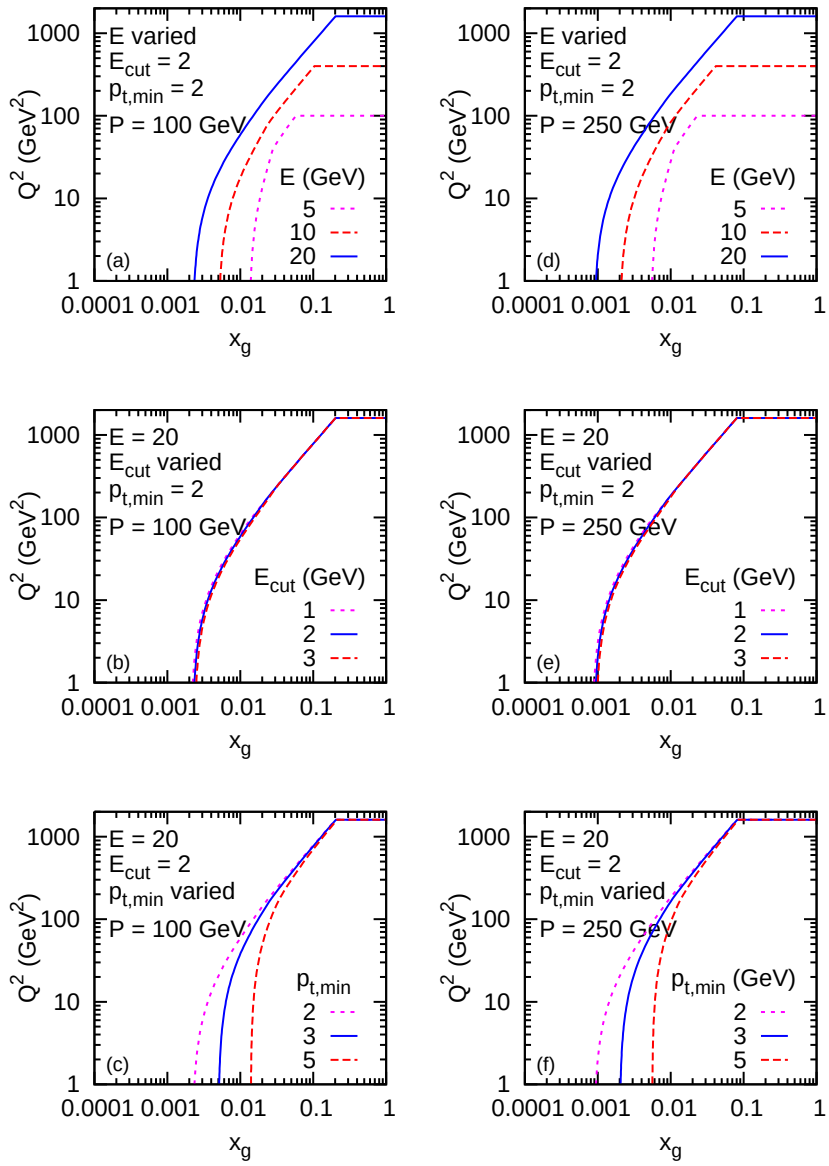

Figure 4: Accessible kinematic range in x_p and Q^2 for the 2+1 jets scenario. The accessible region is plotted for different energies of the beam (100 and 250 GeV for the hadron beam, 5, 10 and 20 GeV for the lepton beam). We also investigate the effects of varying the cuts $E_{\rm cut}$ and $p_{t,\rm cut}$.

The whole message here is that the gluon distribution only enters the structure functions one order later than the quark distribution and thus F_2 will be dominated by the quark distribution. One thus typically constrain the gluon distribution through the DGLAP evolution of the quarks distribution functions. This suffers from two limitations: first, one does not get direct access to the gluon distribution but rather to its convolution with the splitting functions. Then, this will not be related to the quark distribution but to its Q^2-derivative which is less precisely known that the quark distribution itself, especially at small x.

Let us now concentrate on the situations where we impose jets in the final state. As already mentioned, the 1+1-jet case is dominated by the quark distribution and does not present any advantage compared to the inclusive measurement presented above. The case of 2+1 jets is more interesting since the reconstruction of the final state allows to get rid of the convolution present in the inclusive measurements. More precisely, we have

$$\frac{\mathrm{d}^2\sigma_{2+1}}{\mathrm{d}x_p\,\mathrm{d}Q^2} = A_q(x_p,Q^2)\,q(x_p,Q^2)\;+\;A_g(x_p,Q^2)\,g(x_p,Q^2), \tag{22}$$

where the two terms correspond to the quark-initiated and gluon-initiated processes respectively. The coefficients A_q and A_g are matrix elements that can be computed at given order in perturbation theory. They also allow to take into account non-perturbative effects like hadronisation. Note that if various kinematical cuts are applied — like cuts on the energy of the outgoing electron, cuts on its scattering angle or minimal transverse energy for the outgoing jets — the coefficients will probably have to be computed by Monte Carlo.

Even though at small x gluons will dominate over the quark, in general, eq. (22) does not give direct access to the gluon distribution unless we get rid of the contribution proportional to the quark distribution. In what follows, we shall assume that the inclusive measurements give a good enough measurement of the quark distribution so that we can simply assume the quark part in (22) known and subtract it to be left with the gluon-initiated processes. Of course, a more complete approach can include the 2+1-jet cross-section directly in the global QCD fits, determining at the same time the quark and gluon contributions.

A final note concerns the medium effects in e+A collisions. Since the outgoing jets have to travel in the medium, the coefficients A_a and A_g will be affected by in-medium propagation. We shall assume here that the measurements of 1+1-jet cross-sections allow to control how jets propagate in the

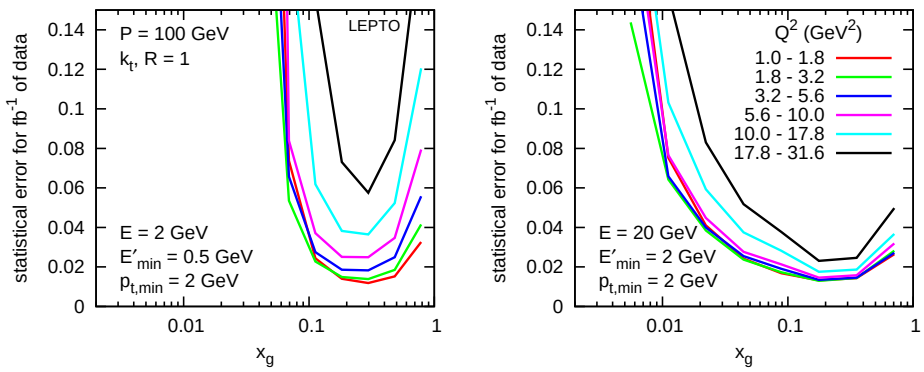

Figure 5: TBA

medium and hence to know the corrections to A_q and A_g. This is not completely trivial as 1+1-jet events will be highly dominated by quark-initiated jets, while in the 2+1-jet case, we can have both quarks and gluons. As a consequence, the medium effects on A_q and A_g will probably introduce an additional systematic error coming from the uncertainty on the gluon-jet propagation[3].

4.3 Simulations and expected statistical errors

In this Section, we estimate the statistical error one may hope to reach at the EIC and compare that to what one may expect from inclusive measurements. For simplicity, we will take the case of $e+p$collisions and run with a hadron-beam energy of 100 GeV. We will discussd in the next Section the expected sources of systematic uncertainties.

Our starting point is the central formula (22). As already mentionned, we shall assume that the quark contribution is given from the inclusive measurements and known. If we further assume that the coefficient A_g is known from Monte-Carlo estimates, the statistical error on the 2+1-jet cross-section directly gives a measure of the statistical error on the gluon distribution.

To estimate the statistical error on the 2+1-jet cross-section, we need to specify the integrated luminosity and fix the kinematic parameters presented in Section 4.1. We will adopt a typical number of 1 fb^{-1} of integrated luminosity, corresponding to about 4 months of data taking at a luminosity

[3]Unless one finds an independent way of studying gluon-jets propagation.

of 10^{32} cm^{-2}s^{-2}. To investigate the effect of the lepton-beam energy, we will consider two situations: a low-energy option of 2 GeV and a high-energy option of 20 GeV. We will impose $E_{\rm cut} = 0.5$ and 2 GeV for the low- and high-energy options, respectively. In both cases, we will impose a $p_{t,\rm cut}$ cut-off on jets of 2 GeV, applied in the Breit frame. Jets have been clustered with the k_t algorithm [3] with a distance parameter $R = 1$ as this is a common choice for DIS experiments.

Practically, we have used LEPTO [4] to generate events and FastJet [5, 6] to perform the jet analysis. We have required exactly 2 jets above $p_{t,\rm cut}$ in the event. In order to minimise the background coming from events with more than two jets or, more importantly, 1+1 jet with a jet coming from the beam remnants passing the p_t threshold, we have imposed on top of the cuts previously introduced, the conditions that the azimuthal angle between the two jets in the Breit frame has to be larger than $\pi - \phi_{\rm cut}$. We fixed $\phi_{\rm cut} = 0.1$, though a complete study of its effects should be made for the real experimental analysis.

Finally, we have studied the 2+1-jet cross-section in bins of x and Q^2. The obtained double-differential cross-section can be translated in a given number of events, given the integrated luminosity. We have chosen to take 12 bins in $\log(Q^2)$ between $Q^2 = 1$ and $Q^2 = 1000$ GeV^2 and 12 bins in $\log(x)$ spanning the kinematic range for x. Since the statistical error is directly given by the square root of the number of events in each bin, one can adapt the statistical error by changing the binning.

The results obtained with this setup are presented in Figure 4.3 for the low-energy option (left plot) and the high-energy option (right plot). In both cases, we see that the statistical error grows at the edges of the phase-space as one might expect. One important point is that, in the bulk of the phase-space, we may reach error of a few percents, *i.e.* comparable to — if not smaller than — the precision obtained in global QCD fits. This means that this dijet measurements can provide a valuable information on the gluon distribution, either by itself, or combined with inclusive measurements.

It is interesting to notice that the uncertainty is minimal at intermediate values. At large x, the statistical uncertainty comes from the fact that partons, especially gluons, carrying a large fraction of teh proton's momentum are rare, *i.e.* has the same origin as the correcponding statistical uncertainty on the structure function measurements. At small x, the main limitation comes from the cuts we had to impose. The most important is certainly the requirements that the jets have a transverse momentum larger than $p_{t,\rm cut}$, as one can see from eq. (16). We thus want to lower $p_{t,\rm cut}$ as much as possible, a challenge that we shall discuss in the next Section.

4.4 Systematic errors

So far, we have only been concerned by the statistical error. Though it is not our aim to give precise estimates for the systematic errors in this note, we shall list in this Section their sources and discuss how one can estimate them in practice. The list presented here is probably not complete but should at least consist in a good starting point for a complete study of this measurement.

First of all, we have to deal with a series of uncertainties related to the fact that dijets may not correspond to the hard process presented in Section 4.2. This is noticeably due to the following list of reasons:

- there is no one-to-one matching between a parton and a jet. There will be corrections due to parton shower and hadronisation. Those corrections will affect the matrix elements in equation (22) and they can be studied, together with their uncertainties using Monte-Carlo techniques. In the same spirit, one can vary the jet definition to study systematic effects due to the clustering. Even though the k_t algorithm with $R = 1$ is the common choice in DIS experiments, varying R may provide valuable information. One can also perform the clustering with different algorithms, like the anti-k_t [7] which defines jets with rigid boundaries, a property that is known to ease the calibration process. Since the efficiency to define jets properly will increase with the p_t of the jet, this question of optimising jet reconstruction is related to the choice of the $p_{t,\mathrm{cut}}$ cut. And we have seen (see Fig. 4) that pushing $p_{t,\mathrm{cut}}$ as low as possible is important if one wants to cover a large region in x.

- the other effect that we want to study is the contamination from events where one of the two hard jets is practically coming from the proton remnants. In this study, we have asked that the two jets are back-to-back within a certain tolerance ϕ_{cut}. Varying the value of that cut-off can certainly give precious information on this background. Another option might be to use the fact that, in the Breit frame, beam renmants and "hard" partons are supposed to be well-separated in rapidity, and then use an additional cut-off in rapidity.

Apart fromn the definition of jets, the other major source of theoretical uncertainty lies probably in the matrix elements $A_{q,g}$. In this study, they have been determined by Monte-Carlo and we have already mentioned that parton showers and hadronisation will affect them. Using different Monte-Carlo generators, varying the cuts and using different input PDF sets are

as many methods that can be used to extimate the uncertainties on those matrix elements. The other source of theoretical uncertainty is the choice of the scale for the partonic distributions in (22): here we have used Q^2 which is most likely valid when Q is tha hard scale in the process. But at smaller Q^2, something proportional to $p^2_{t,\mathrm{cut}}$ should be more appropriate.

On top of that, there will be a series of more experimental uncertainties. Among them, the most obvious is probably the one characterised by the requirement that the energy of the scattered electron is larger than E_{cut}. The detection of this electron might for example be more difficult close to the beam and, as a consequence, we may also want to impose a cut on its scattering angle. Similarly, all the clustering has been done in the Breit frame and we have discussed methods which allows clean separation between the beam remnants and the hard partonic process. Even though we have already impose cuts to gain confidence that the two reconstructed jets are coming from the partonic process, going from the laboratory frame to the Breit frame might be experimentally challenging, especially in some regions of the phase-space that involve large boosts.

4.5 Conclusions and discussion

Let us conclude this study of the gluon distribution by summarising our results and discussing a few points that have been left apart in the previous parts.

We have seen that the study of the differential dijet cross-section allows a direct access to the gluon density. We have estimated that this method for extracting the gluon density has relatively small statistical uncertainties, especially at intermediate values of x.

The main message is thus that this measurement can provide valuable information of the gluon density, if not on its own, at least by combining it with DGLAP fits of the inclusive structure function measurements.

The main motivation for using jets to access the gluon density comes from two facts: first, for simple systems, *i.e.* 1+1 jet events, the gluon is suppressed by a power of the strong coupling conpared to the quark and, second, by measuring the dijet invariant mass, one can reconstruct the incoming parton. THhe whole discussion have been carried on at the leading order of the perturbation theory. Since most of the global QCD fits used to extract the gluon density are doing so at next-to-leading order (NLO) or event at NNLO, it is legitimate to ask if this approach survives beyond leading order. Obviously, the matrix elements A_q and A_g would suffer corrections in α_s due tu extra radiation inside the jets. But on top of that, we

may have contamination from 3-jet events. However, the requirement that the two hard jets are nearly back-to-back surely helps selecting a clear dijet sample and limits the sensitivity to NLO corrections. Further studies of the $\phi_{\rm cut}$ dependence would help understanding this more quantatively.

References

[1] V.N. Gribov and L.N. Lipatov, *Sov. J. Nucl. Phys.* **15** (1972) 438; G. Altarelli and G. Parisi, *Nucl. Phys.* **B126** (1977) 298; Yu.L. Dokshitzer, *Sov. Phys. JETP* **46** (1977) 641.

[2] S. Moch, J. A. M. Vermaseren and A. Vogt, *Nucl. Phys. B* **688** (2004) 101 [`hep-ph/0403192`]; A. Vogt, S. Moch and J. A. M. Vermaseren, *Nucl. Phys. B* **691** (2004) 129 [`hep-ph/0404111`].

[3] S. Catani, Y. L. Dokshitzer, M. H. Seymour and B. R. Webber, *Nucl. Phys.* **B406** (1993) 187; S. Catani, Y. L. Dokshitzer, M. Olsson, G. Turnock and B. R. Webber, *Phys. Lett.* **B269** (1991) 432; S. D. Ellis and D. E. Soper, *Phys. Rev.* **D48** (1993) 3160 [`hep-ph/9305266`].

[4] G. Ingelman, A. Edin and J. Rathsman, *Comput. Phys. Commun.* **101** (1997) 108 [`hep-ph/9605286`].

[5] M. Cacciari, G. P. Salam, and G. Soyez, "FastJet," `http://www.fastjet.fr`.

[6] M. Cacciari and G. P. Salam, *Phys. Lett.* **B641** (2006) 57 [`hep-ph/0512210`].

[7] M. Cacciari, G. P. Salam and G. Soyez, JHEP **0804** (2008) 063 [`arXiv:0802.1189`].